

# Theoretical and Computational Study on Swept Back Wing for Variable Mach Ranges

Avish Lamsal<sup>1</sup>, Ankit Kumar Mishra<sup>3</sup>, Sheetal Prajapati<sup>2</sup>, Jonathan William<sup>1</sup>

<sup>1</sup>Graduate Research Trainee, Department of Research and Development, ASTROEX RESEARCH ASSOCIATION, Deoria, India

<sup>2</sup>Junior Research Fellow, Department of Research and Development, ASTROEX RESEARCH ASSOCIATION, Deoria, India

<sup>3</sup>Research Supervisor, Department of Research and Development, ASTROEX RESEARCH ASSOCIATION, Deoria, India

---

## ABSTRACT

**In this work, numerical simulations on swept back wing for variable Mach ranges are performed for the airflow through the SELIG 1223 airfoil. SolidWorks is used for Modelling of the wing. ANSYS is used for domain generation and meshing and FLUENT is used as a solver. The aerodynamic performance of the numerical simulation for airfoil S1223 are presented in terms of lift and drag coefficients compared for a range of Angle of Attack, Variable Mach Numbers, Velocity and Pressure distributions for the chord based Reynolds number of  $2 \times 10^5$ . These aerodynamic characteristics can provide a useful reference for the aerodynamic layout design and dynamic analysis of the variant aircraft.**

**Keywords: Angle of Attack, Coefficient of lift, Coefficient of drag, K-omega SST, SolidWorks, S1223 Airfoil.**

---

## 1. INTRODUCTION

The design and analysis of the wings of aircraft is one of the principal applications of the science of aerodynamics. The prediction of aerodynamic characteristics of an airfoil is still a challenging task, in spite of recent developments in Computational Fluid Dynamics. The main concern in aerodynamics is about the forces applied by air molecules on an object's surfaces which results from the air's flow with respect to that object. Its performance and stability during flight are determined by these forces and the moment they produce around its centre of gravity. The net force produced by the sum of these forces exerted by moving air molecules on an object's surface can be divided into two parts: lift force and drag force. Every shape of object experiences a sizable amount of drag from airflow; however for the majority of shapes, lift is little until the flow velocity is high. The relationship between these aerodynamic forces and the angle of attack of the wing, and consequently the performance of the wing, is determined by the shape of the wing's cross-section. This implies that the aerodynamic performance characteristics of wings with various airfoil cross sections vary. Selig and Guglielmo created the low Reynolds number, high lift S1223 airfoil, which they experimentally tested at a Re number of  $2 \times 10^5$ . Increased payloads, shorter takeoff and landing distances, lessened aircraft noise, and lower stall speeds are just a few of the challenges that modern applications must address. The advantages of improved low Reynolds airfoil aerodynamics suitable for high-lift conditions represent the solutions for many of these applications.

## 2. LITERATURE REVIEW

Trong T. Bui (2018) conducted a CFD analysis to assess the high-speed aerodynamics for airworthiness of the swept wing of a Gulfstream GIII airplane (Gulfstream Aerospace Corporation, Savannah, Georgia). It was discovered that the inboard trailing-edge modification device had a negative impact on the aerodynamics of the flow in the outboard area of the wing in front of the aileron [1]. Su Xinbing et al (2019) studied on the Influence of Swept Angle on the Aerodynamic Characteristics of the Cross-Section Airfoil of a Variable Swept-Wing Aircraft. When the angle of attack changes the drag coefficient of each airfoil increases with the increase of the forward sweep angle as well as the lift coefficient decreases with the increase of the forward sweep angle for the cross-sectional airfoil with larger relative thickness. When the Mach number changes, the cross-section airfoils lift coefficient declines as the forward sweep angle rises, and the cross-section airfoils drag coefficient similarly rises as the forward sweep angle rises [2]. A study on the Low-Speed and High Angle of Attack Aerodynamic Characteristics of Supersonic Business Jet with Forward Swept Wing was conducted by Nao Setoguchi et al. in 2020. Numerical findings show that the Forward Swept wing (FSW) had different stall characteristics than the Backward Swept Wing (BSW) despite having a high angle of attack,

the outboard vortex and the outboard trailing-edge vortex developed negative pressure on the upper surface of the wing. Which results, the vortices at high angles of attack enable the FSW to produce a lift force [3]. Charalampos Papadopoulos et al (2021) worked a 3D numerical study on the influence of the span wise distribution of tubercles on an unmanned aerial vehicle wing. Based on the UAVs wing mean chord, the results indicate that there is a noticeable possibility for managing the flow on the UAVs wings, which could result in an improvement in aerodynamic performance and efficiency [4]. Khan et al (2022) investigated and compared the wing planform's effect on the aerodynamic parameters of aircraft wings using computational fluid dynamics (CFD). A rectangular wing has a high lift and drag coefficient among all the wing planforms, there will be no lift generation for symmetric airfoil at an angle of attack (AoA) of 0°. The sweptback wing has nearly the same or a little effect on the values of lift and drag coefficient. Taper ratio is most effective planform parameter which not only improve the aerodynamic characteristics to a greater extent but there is also weight reduction [5]. Mohammad Sadegh Salari et al (2018) in his paper entitled Aerodynamic Analysis of Backward Swept in Horizontal Axis Wind Turbine (HAWT) Rotor Blades Using CFD said that the aerodynamics of flow around the wind turbine blades plays an important role on wind turbine efficiency. At lower wind velocities, the output power and the axial thrust of the rotor decrease whereas at the higher wind velocities the output power increases while the axial thrust decreases. Backward swept blade is a better configuration for increasing the power at moderate and high wind speeds as it reduces aerodynamic loads on the rotor and increase blade efficiency [6]. Kovalev M.A et al (2019) presented a paper on the topic choosing the aerodynamic configuration of a subsonic cruise missile where comparison of two aerodynamic configurations on subsonic cruise missiles with a moderately swept wing have similar aerodynamic characteristics. Missiles with swept-back wings have better aerodynamic performance in terms of maximum aerodynamic quality, while the lift increment due to reduced trim losses for the forward-swept wing configuration only partially compensates the difference of the aerodynamic characteristics of the alternatives [7]. Yuchang Lei et al (2020) they have conducted a Numerical Study on Aerodynamic Characteristics of Variable-sweep Morphing Aircraft at Transonic Speeds. Under the subsonic condition, a small sweepback has a greater impact on the lift. Under the transonic condition a large sweepback has a greater impact on the lift. For a given Mach number, the drag coefficient decreases when the sweepback increases. For a given sweepback, when the Mach number increases, the drag first increases and then decreases. On the other hand, Altitude has a low influence on lift coefficient, but a large influence on drag coefficient at subsonic speeds [8]. Radhakrishnan P et al (2021) studied on Aerodynamic Performance Analysis of a Variable Sweep Wing for Commercial Aircraft Applications. Their results show that at low speed (Mach=0.8) straight wing has high L/D ratio and at the sonic speed (Mach=1) sweep wing has higher L/D ratio and in Supersonic Speed (Mach=1.2) delta wing tends to have higher L/D ratio [9]. Bei Lui et al (2022) conducted Surrogate-based aerodynamic shape optimization of a morphing wing considering a wide Mach-number range. Morphing wing is a promising technology to address in the field of aerospace. These studies indicated that optimized morphing wing features a very good aerodynamic performance improvement over the flow regimes from subsonic to hypersonic flow conditions [10].

### 3. METHODOLOGY

#### 3.1 Numerical Analysis

The main aim of the investigation is to design wing which generates high lift and low drag to reduced fuel consumptions. For the outer profile of the wing, S1223 airfoil was considered in this study. However, these investigations are carried out at a lower Re of  $2 \times 10^5$ . The air density ( $\rho$ ) is  $1.225 \text{ kg/m}^3$  and its dynamic viscosity ( $\mu$ ) of  $1.7894 \times 10^{-5} \text{ kg/m-s}$ . The fluent turbulence model of k- $\omega$  SST with two-equation was used. The k- $\epsilon$  model is the turbulent flow model and assumes that the molecular viscosity effect is minimal. The transport equation was derived by using the assumption. This model is valid for fully developed turbulent flow only. While the SST K- $\omega$  assumes that the turbulent flow viscosity is changing. The turbulent viscosity of fluid is varying to account for the transfer of the primary turbulent shear stress. By comparing the SST K- $\omega$  model to the K- $\omega$  model, this changing flow viscosity gives an advantage to SST K- $\omega$  over both the standard k- $\omega$  model and the standard k- $\epsilon$  model. The transport equation of SST k -  $\omega$  model is given by [5].

$$\frac{\partial}{\partial t}(\rho K) + \frac{\partial}{\partial x_i}(\rho k u_i) = \frac{\partial}{\partial x_j} \left( \Gamma_k \frac{\partial k}{\partial x_j} \right) + G_k - Y_k + S_k \quad (1)$$

$$\frac{\partial}{\partial t}(\rho \omega) + \frac{\partial}{\partial x_i}(\rho \omega u_i) = \frac{\partial}{\partial x_j} \left( \Gamma_\omega \frac{\partial \omega}{\partial x_j} \right) + G_\omega - Y_\omega + S_\omega + D_\omega \quad (2)$$

Where effective diffusivity of K and  $\omega$  are  $\Gamma_K$  and  $\Gamma_\omega$  the respectively.  $Y_k$  and  $Y_\omega$  represent the dissipation of K and  $\omega$  due to turbulence and  $D_\omega$  represents the cross-diffusion term.  $S_k$  and  $S_\omega$  are user defined source terms.  $G_k$  represents the generation of turbulence kinetic energy due to mean velocity gradients and  $G_\omega$  represents the generation of  $\omega$ . The boundary condition for the investigation is:

- a. Airfoil is considered as solid-wall with no-slip condition.
- b. The inlet of the fluid domain is assigned as velocity inlet.
- c. The outlet of the fluid domain is pressure.

### 3.2 Aerodynamic Parameters

The main aerodynamic parameters of the wing are the lift (Cl) drag (Cd) coefficients, lift (Fl) and drag (Fd) forces and the airfoil efficiency (Cl/Cd). A fluid flowing around an airfoil can exert a force on it. This force can be resolved into two components, lift force and drag force as shown in figure. Fl is the component that is normal to the fluid flow. The airfoil shape is design so that it generates a pressure difference between up and lower surface flow, due to which lift is generated. Fl is acting upward to counter the effect gravity, although it can be acting in any direction normal to the fluid flow. In contrast, the Fd is the component that is acting parallel to the fluid flow. Drag force is acting in opposite direction to the fluid velocity. The Cd is the sum of zero-lift drag (Cdo) and the induced drag (Cdi). The ratio of lift (Cl) to drag coefficient (Cd) determines the aerodynamic performance of the wing. The Cl /Cd shows the amount of lift generated by an airfoil to its drag. The Cl/Cd ratio represents the efficiency or performance of the airfoil. The Cl/Cd determine the stall angle where the wing efficiency is maximum.

$$C_d = C_{d0} + C_{di} \quad (3)$$

$$C_d = \frac{2FD}{\rho AV^2} \quad (4)$$

$$C_l = \frac{2Fl}{\rho AV^2} \quad (5)$$

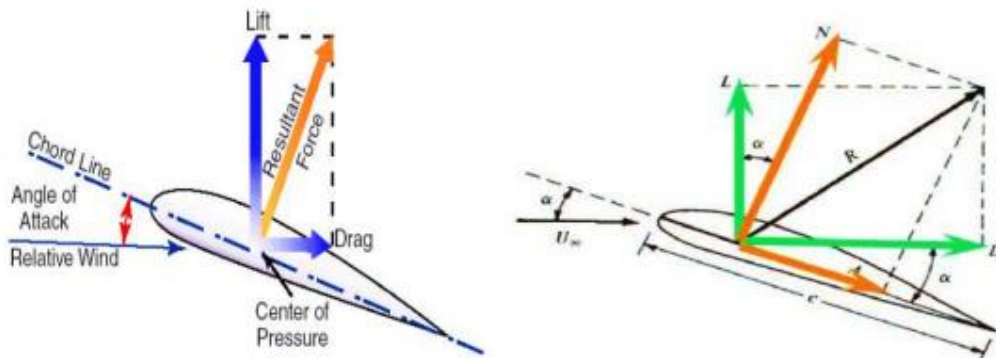


Figure 1. The force distribution on the airfoil [5]

### 4. GEOMETRY

A wing prototype (Fig. 2) was constructed using SolidWorks and it was exported to ANSYS for creating a mesh and computational domain. The wing is the swept wing which has wing tip of 0.3 m and chord length of 0.5 m.

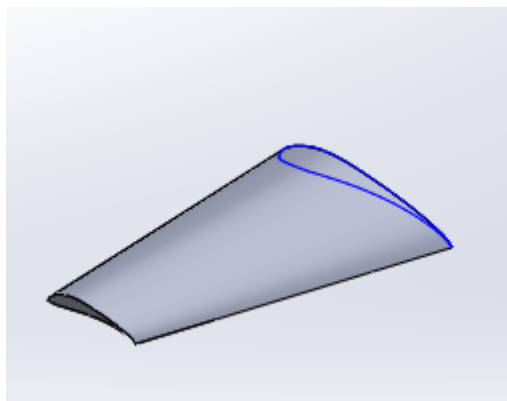


Figure 2: Wing Geometry

## 5. DOMAIN GENERATION

The geometry of the computational domain is depicted in the image below. The rectangular part is 5 m long and has a length of 4m for the semi-circular segment. The 1m chord length airfoil is positioned in the domain so that its trailing edge is near the centre of the diameter of the domain's semi-circular area and that its chord-line corresponds with the domain's symmetry line. When there was a flow moving at a speed of 10 m/s, the velocity inlet boundary condition was used. The outlet boundary condition was used similarly for the outflow. Other borders were subject to the wall requirement. The flow velocity's sine component is parallel to the y-axis of the domain, whereas the cosine component is parallel to the x-axis. The turbulence intensity for the velocity inlet boundary condition is taken into account to be 0.5% for this study since it is expected that the inflow turbulence is relatively low compared to the outflow.

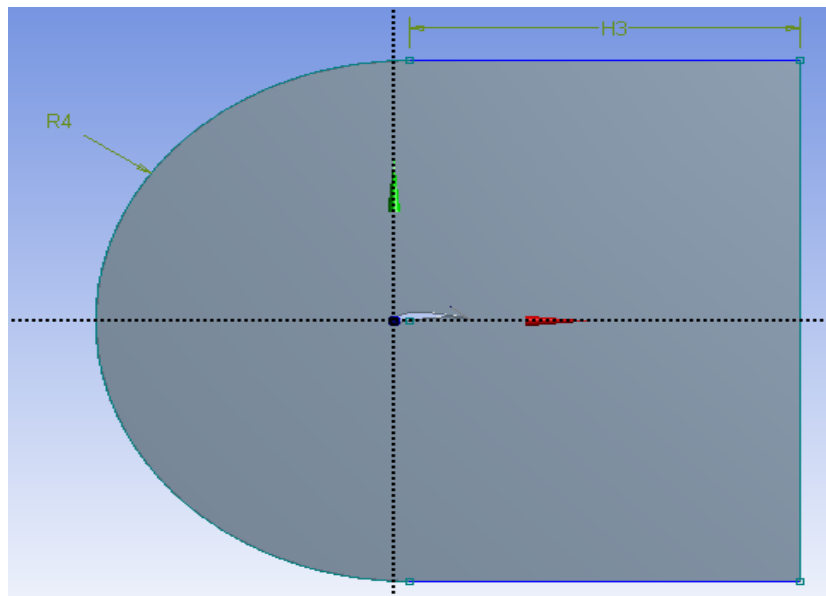


Figure 3: The dimensions and boundary conditions of the computational domain

## 6. MESHING

The ANSYS Meshing component was used to create the meshes. A C-type grid structured mesh was created, and the result is depicted in the figure below. It was determined that the mesh quality was ideal having nodes 42944 and elements 83596. The boundary conditions, turbulence model, and other options were chosen after importing the meshes into the fluent solver.

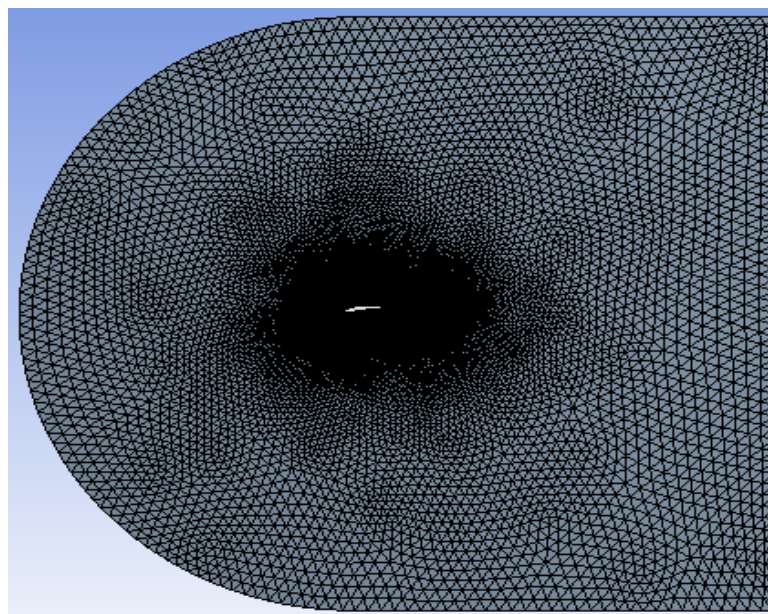


Figure 4: C-mesh Fluid Domain

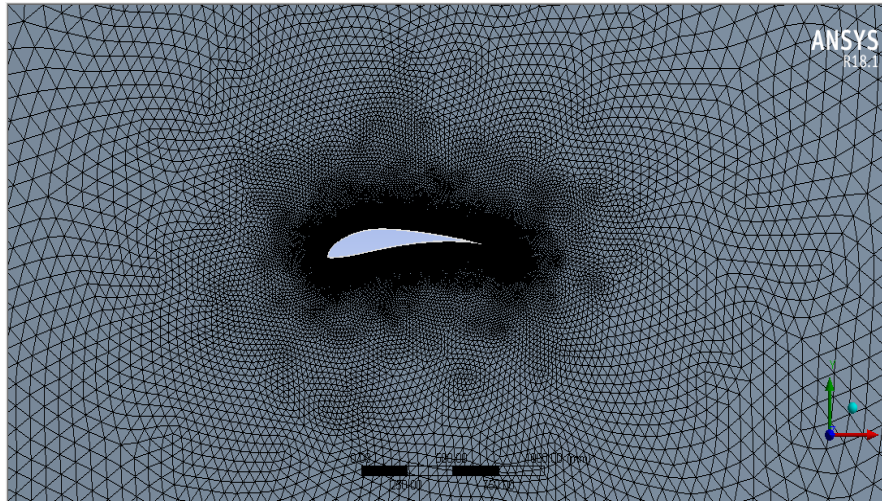


Figure 5: body of influence sizing function centred on the airfoil

### 7. PROCESSING ON FLUENT AND SELECTION OF TURBULENCE MODEL

The creation of a turbulence model entails using mathematical models to foretell how turbulence will affect an aerofoil. For RANS equations, the K-model, a two-equation turbulence model, is employed. It makes use of two variables, kinetic energy (k) and specific rate of dissipation ( $\omega$ ). This model is integrated with the widely utilized SST model, which represents shear stress transport.

On FLUENT, the input parameters and the particular circumstances listed in the table below were provided.

<b>Solver</b>	Pressure based steady
<b>Viscous Model</b>	k- $\omega$ SST model
<b>Density (kg/m<sup>3</sup>)</b>	1.225
<b>Viscosity(kg/m-s)</b>	0.0000179
<b>Turbulence intensity ratio</b>	0.05
<b>Turbulence length scale</b>	1m
<b>Inlet Velocity(m/s)</b>	10
<b>Reynolds Number</b>	$2 \times 10^5$
<b>Chord Length(m)</b>	1m
<b>Momentum</b>	Second order Upwind
<b>Pressure velocity coupling</b>	Coupled

### 8. RESULTS AND DISCUSSION

Pressure contour:

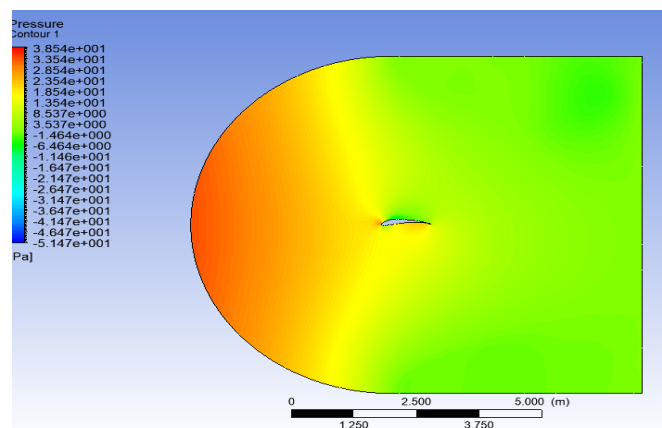
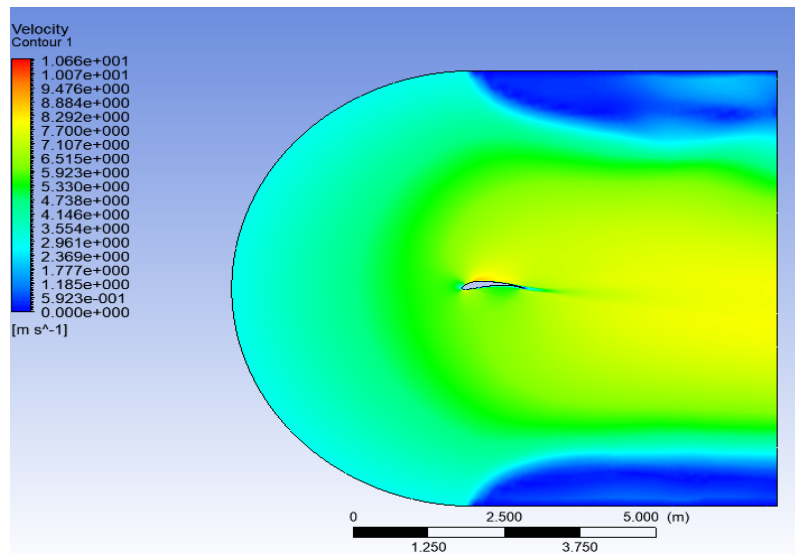


Figure 6: Pressure distribution contour diagram of airfoil S1223

**Velocity Contour:**



**Figure 7: Velocity distribution contour diagram of airfoil S1223**

**Comparison Plots of Aerodynamic Force Coefficients:**

As shown below is the chart of the airfoil coefficient of lift (Cl) vs angle of attack ( $\alpha$ ) and coefficient of drag (Cd) vs. angle of attack ( $\alpha$ ). It can be observed how lift and drag coefficients change in relation to angle of attack. The stall angle for a given airfoil is the Angle of Attack at which the highest Coefficient of Lift (Cl max) value is obtained

**Table 1: Coefficient of Lift, Drag of S1223 airfoil at different Angles of Attack**

Angle of attack( $\alpha$ )	Coefficient of Lift (Cl)	Coefficient of Drag (Cd)	Cl/Cd
0	0.89742	0.023038	38.95390225
2	1.0038	0.041123	24.40969774
4	1.1029	0.062531	17.63765172
8	1.2907	0.11385	11.33684673
10	1.3757	0.14294	9.624317896
12	1.4547	0.17388	8.366114562

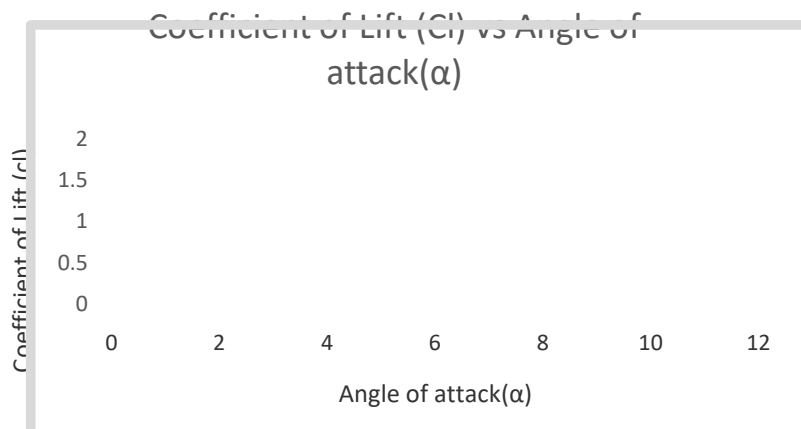


**Figure 8: Coefficient of lift vs Angle of attack**

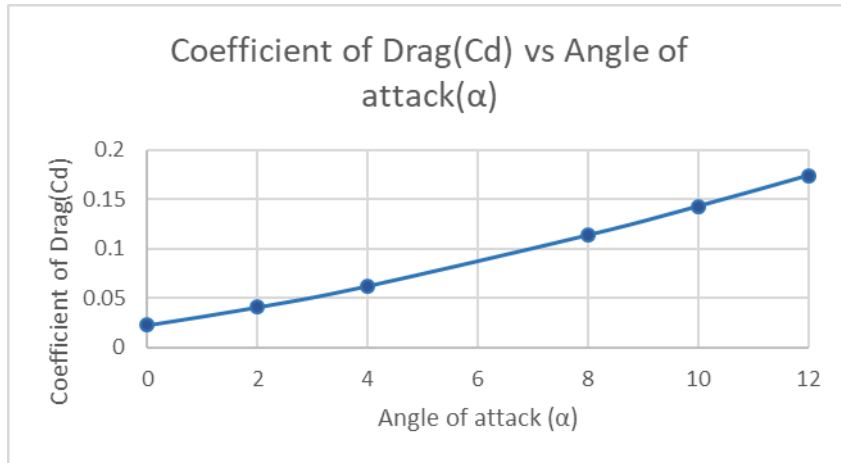


Figure 9: Coefficient of drag vs Angle of attack

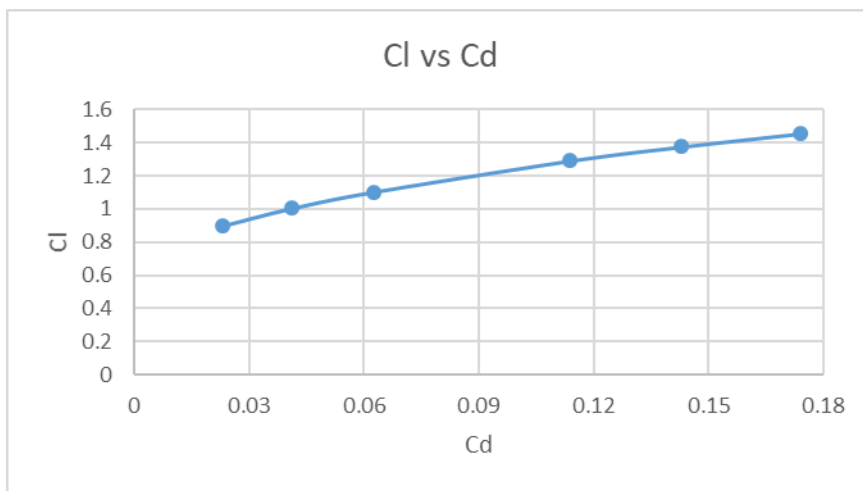


Figure 10: Coefficient of drag vs Coefficient of lift

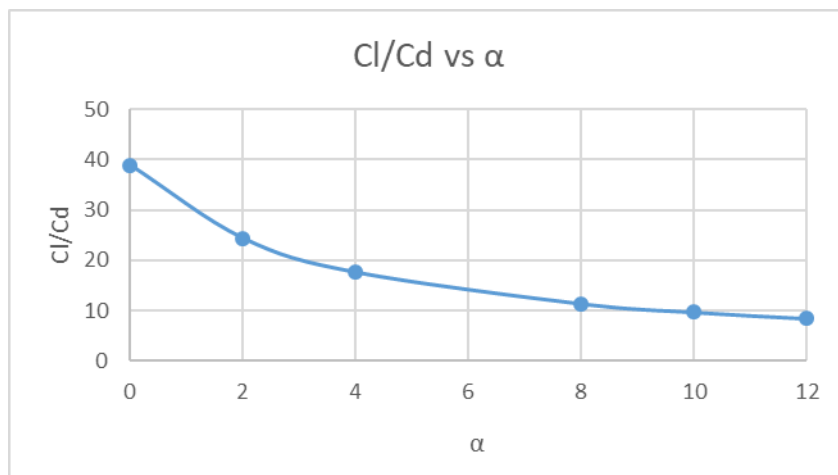


Figure 11: Ratio of Coefficient of lift, Coefficient of drag vs Angle of attack

**Comparison Plots of Variable Mach Numbers**

The Mach number is the ratio of flow velocity after a certain limit of the sound's speed. In simple words, it is the ratio of the speed of a body to the speed of sound in the surrounding medium. The significant of Mach number is that the airflow has higher speeds than the sound.

$$M = v/c \tag{6}$$

Where, M is Mach number, v is object speed and c is speed of sound.

**Table 2: Various regimes of Mach values**

Regime	Subsonic	Transonic	Sonic	Supersonic	Hypersonic	Hypervelocity
Mach	<0.8	0.8–1.3	1.0	1.3–5.0	5.0–10.0	>10.0

The table and charts of varied Mach numbers are displayed below. Using the speed of sound (c), which is 343 m/s, as the starting point, several Mach numbers of various regimes were selected to determine the value of object speed (v).

**Table 3: Object speed at different Mach Numbers**

Mach Number	Speed of sound (c)	Object speed(v)
0	343m/s	0m/s
1	343m/s	343 m/s
3	343m/s	1029 m/s
6	343m/s	2058 m/s
8	343m/s	2744 m/s
9.5	343m/s	3259 m/s
12	343m/s	4116 m/s

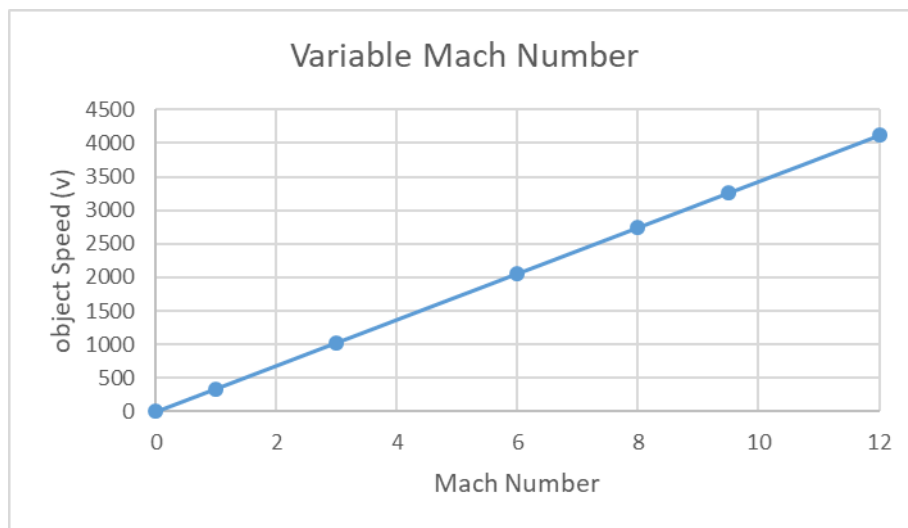


**Figure 12: Mach number Vs Object Number**

### CONCLUSION

**From the above numerical simulation data diagrams, some conclusions can be obtained as follows:**

- From Fig 6 and Fig 7 it can be observed that pressure generated on the tip of airfoil is more than other surface and the velocity generated on the upper surface of airfoil is more.
- From Fig 8 and Fig 9, when the angle of attack increases coefficient of lift, drag increases as well as it can be clear from Fig 8 that S1223 is high lift airfoil.
- From Fig 10, The value of Cl is greater than the Cd, When the coefficient of lift increases Coefficient of drag also increases,
- From Fig 11, when the angle of attack increases the ratio of coefficient of lift and drag decreases as the lift-to-drag ratio is influenced greatly by the Reynolds number, that is the lift-to-drag ratio decreases with the reduction of Reynolds number.
- From Fig 12 it can be clear that more the Mach number more the object speed, at subsonic speeds, altitude has little effect on the lift coefficient but a lot on the drag coefficient. The variable swept-back rule should be



modified when examining it in order to account for the effect of height on aerodynamic properties at subsonic speeds.

- f. Thus, the ideal sweepback rises with the increase in Mach number when the lift-drag ratio is chosen as the index to quantify aerodynamic gains; however there is no linear relationship between the optimal sweepback and Mach number.

#### REFERENCES

- [1] T. T. Bui, "Analysis of High-Speed Aerodynamics of a Swept Wing with Seamless Flaps," in *Applied Aerodynamics Conference*, Atlanta, Georgia, 2018.
- [2] J. W. a. Z. X. Su Xinbing, "Study on the Influence of Swept Angle on the Aerodynamic Characteristics of the Cross-Section Airfoil of a VariableSwept-Wing Aircraft," in *IOP Conference Series: Materials Science and Engineering*, College of Aeronautical Engineering, Air Force Engineering University, Xi'an 710038, china, 2019.
- [3] M. K. Nao Setoguchi, "Low-Speed and High Angle of Attack Aerodynamic Characteristics of Supersonic Business Jet with Forward Swept Wing," in *AIAA SciTech Forum*, 2020, Orlando, FL , 2020.
- [4] V. K. Y. Charalampos Papadopoulos, "Influence of tubercles' spanwise distribution on swept wings for unmanned aerial vehicles," *Journal of aerospace engineering*, p. 9, 2021.
- [5] M. S. M. ., J. T. J. Salman Khan, "To investigate and compare the wing planform's effect on the aerodynamic parameters of aircraft wings using CFD," p. 17, 2022.
- [6] B. Z. B. M. B. Mohammad Sadegh Salari, "Aerodynamic Analysis of Backward Swept in HAWT Rotor Blades Using CFD," *Int.Journal ofRenewable Energy Development*, pp. 241-249, 2018.
- [7] k. M. N. A.N., "Choosing the aerodynamic configuration of a subsonic cruise missile," *Samara National Research University*, pp. 59-66, Vol 18, No 3 (2019).
- [8] R. G/. G. H. ., C. 2. a. C. A. N. Radhakrishnan P, "Aerodynamic Performance Analysis of a Variable Sweep Wing for Commercial Aircraft Applications," *ACS Journal for Science and Engineering*, pp. 31-37, Vol. 1 - No. 1 2021.
- [9] H. I. Z. H. H. G. Y. Bei Liu, "Surrogate-based aerodynamic shape optimization of a morphing wing considering a wide Mach-number range," *Aerospace science and technology*, p. Volume 124, May 2022.